Molecular Phylogenetics and Evolution 151 (2020) 106901

Contents lists available at ScienceDirect

Molecular Phylogenetics and Evolution

journal homepage: www.elsevier.com/locate/ympev

Plastome phylogenomics, systematics, and divergence time estimation of the *Beilschmiedia* group (Lauraceae)

Haiwen Li[a,c], Bing Liu[a], Charles C. Davis[b,*], Yong Yang[a,*]

[a] State Key Laboratory of Systematic and Evolutionary Botany, Institute of Botany, the Chinese Academy of Sciences, Beijing 100093, China
[b] Department of Organismic and Evolutionary Biology, Harvard University Herbaria, 22 Divinity Avenue, Cambridge, MA 02138, USA
[c] University of the Chinese Academy of Sciences, Beijing, China

ARTICLE INFO

Keywords:
Beilschmiedia group
Lauraceae
Molecular clock
Plastome
Phylogenomics
Systematics

ABSTRACT

Intergeneric relationships of the *Beilschmiedia* group (Lauraceae) remain unresolved, hindering our understanding of their classification and evolutionary diversification. To remedy this, we sequenced and assembled complete plastid genomes (plastomes) from 25 species representing five genera spanning most major clades of *Beilschmiedia* and close relatives. Our inferred phylogeny is robust and includes two major clades. The first includes a monophyletic *Endiandra* nested within a paraphyletic Australasian *Beilschmiedia* group. The second includes (i) a subclade of African *Beilschmiedia* plus Malagasy *Potameia*, (ii) a subclade of Asian species including *Syndiclis* and *Sinopora*, (iii) the lone Neotropical species *B. immersinervis*, (iv) a subclade of core Asian *Beilschmiedia*, sister to the Neotropical species *B. brenesii*, and v) two Asian species including *B. turbinata* and *B. glauca*. The rampant non-monophyly of *Beilschmiedia* we identify necessitates a major taxonomic realignment of the genus, including but not limited to the mergers of *Brassiodendron* and *Sinopora* into the genera *Endiandra* and *Syndiclis*, respectively. Along these lines, the high degree of continental, clade-wide endemism we identify suggests that geographical distribution may be a good proxy for delineating taxa within this group. Our molecular divergence time estimates indicate that stem *Beilschmiedia* group members date to the Early Eocene (~50 Ma); their crown age dates to the Eocene–Oligocene boundary (~34 Ma). These findings contradict older estimates of the group and support mounting evidence that the origin and diversification of many pantropical angiosperm clades are not easily attributed to strict western Gondwanan vicariance. Finally, our study highlights the phylogenetic utility of plastomes in Lauraceace, and lays a solid foundation for future phylogenomic and biogeographic investigations within the family.

1. Introduction

Members of the angiosperm family Lauraceae are widely distributed across the tropics and are especially diverse in Asia and the Americas (Gentry, 1988; Rohwer, 1993; Sri-Ngernyuang et al., 2003). They represent ecologically dominant woody elements, especially in tropical forests, and are utilized by humans for various purposes including timber [e.g., *Phoebe nanmu* (Oliv.) Gamble], spices (e.g., *Cinnamomum aromaticum* Nees), food (e.g., *Persea americana* Mill.), and medicine [e.g., *Lindera aggregata* (Sims) Kosterm.] (Rohwer, 1993; Zhang and He, 2014; Ning and Xing, 2014). Despite the ecological and economic importance and ongoing efforts to resolve the phylogeny of Lauraceae (e.g., Rohwer, 2000; Chanderbali et al., 2001; Rohwer and Rudolph, 2005; Li et al., 2004, 2011; Rohwer et al., 2014; Huang et al., 2016; Rohde et al., 2017), numerous systematic questions within the family remain unresolved.

Relatively little focused attention has been given to *Beilschmiedia* Nees and its closest relatives (i.e., hereafter referred to as the *Beilschmiedia* group). The *Beilschmiedia* group belongs to tribe Cryptocaryeae and shares several diagnostic features including wood anatomy (Richter, 1981), inflorescence type (van der Werff and Richter, 1996), and molecular phylogenetic data (Chanderbali et al., 2001; Rohwer and Rudolph, 2005; Rohwer et al., 2014). Kostermans (1957) first recognized the *Beilschmiedia* group (as 'subtribe Beilschmiediineae', tribe Perseeae) to include the following genera: *Apollonias* Nees, *Dehaasia* Bl., *Mezilaurus* Taub., *Beilschmiedia*, *Endiandra* R. Br., *Hexapora* Hook. f., and *Potameia* Thouars (including *Syndiclis* Hook. f.). Rohwer (1993), in contrast, felt that the first three genera instead belonged to the *Persea* group, and thus excluded them thereby restricting the *Beilschmiedia* group to include only *Beilschmiedia*, *Endiandra*,

* Corresponding authors.
E-mail addresses: cdavis@oeb.harvard.edu (C.C. Davis), 710309338@qq.com (Y. Yang).

https://doi.org/10.1016/j.ympev.2020.106901
Received 4 December 2019; Received in revised form 6 May 2020; Accepted 26 June 2020
Available online 30 June 2020

Table 1
Vouchers and accession no. of species of the *Beilschmiedia* group sampled for this study.

Latin Name	Collection	Locality	Herbarium	Accession No.
Beilschmiedia appendiculata (Allen) S.K. Lee & Y.T. Wei	Bing Liu 1504	China: Guangdong	PE	MT720932
B. brachythyrsa H.W. Li	Bing Liu 2525	China: Yunnan	PE	MT720931
B. brenesii C.K. Allen	S. Yasuda 1310	Costa Rica	MO	MT720933
B. brevipaniculata C.K. Allen	Bing Liu 1807	China: Hainan	PE	MT720934
B. brunnea B. Hyland	B. Gray 8821	Australia: Queensland	MO	MT720935
B. delicata S.K. Lee & Y.T. Wei	Bing Liu 1632	China: Yunnan	PE	MT720936
B. fasciata H.W. Li	Bing Liu 2468	China: Yunnan	PE	MT720937
B. glauca S.K. Lee & L.F. Lau	Bing Liu 1810	China: Hainan	PE	MT720938
B. immersinervis Sach. Nishida	S. Yasuda 1312	Costa Rica	MO	MT720939
B. obtusifolia (F. Muell. ex Meisn.) F. Muell.	B. Gray 8845	Australia: Queensland	MO	MT720940
B. pergamentacea C.K. Allen	Bing Liu & Yong Yang 2026	China: Yunnan	PE	MT720941
B. pierreana Robyns & R. Wilczek	SIMAB 12,418	Gabon	MO	MT720942
B. purpurascens H.W. Li	Bing Liu 1443	China: Yunnan	PE	MT720955
B. rufohirtella H.W. Li	Bing Liu 1493	China: Yunnan	PE	MT720943
B. tooram (F.M. Bailey) B. Hyland	B. Gray 8763	Australia: Queensland	MO	MT720944
B. yunnanensis Hu	Bing Liu 1645	China: Yunnan	PE	MT720945
Endiandra microneura C. White	B. Gray 8787	Australia: Queensland	MO	MT720946
E. monothyra subsp. *monothyra* B. Hyland	B. Gray 8839	Australia: Queensland	MO	MT720947
E. montana C. White	B. Gray 8872	Australia: Queensland	MO	MT720948
E. xanthocarpa B. Hyland	B. Gray 8813	Australia: Queensland	MO	MT720949
Potameia microphylla Kosterm.	Z.D. Chen, Bing Liu & J.F. Ye 29,875	Madagascar: Antsohihy	MO	MT720950
Sinopora hongkongensis (N.H. Xia et al.) J. Li et al.	Bing Liu 1828	China: Hong Kong	PE	MT720951
Syndiclis fooningensis H.W. Li	Bing Liu 1496	China: Guangxi	PE	MT720952
S. kwangsiensis (Kosterm.) H.W. Li	Bing Liu 1552	China: Guangxi	PE	MT720953
S. sp.	Bing Liu, Q.W. Lin & L. Jiang 2134	China: Yunnan	PE	MT720954

Brassiodendron C.K. Allen, *Hexapora*, and *Potameia* s.l. (including *Syndiclis*). In the most recent classification we adopt here (van der Werff and Nishida, 2010; Yang et al., 2012; Liu et al., 2013; Rohwer et al., 2014), the group is monophyletic and consists of seven genera: *Beilschmiedia*, *Endiandra* (including *Brassiodendron* and *Triadodaphne* Kosterm.), *Hexapora*, *Potameia*, *Sinopora* J. Li et al., *Syndiclis*, and *Yasunia* van der Werff. The members of this group are markedly different from other species of tribe Cryptocaryeae owing to their fruits, which are not enclosed in a receptacular tube (vs. fruits enclosed in a receptacular tube in other Cryptocaryeae, Rohwer et al., 2014).

The *Beilschmiedia* group is pantropically distributed and includes nearly 400 species. *Beilschmiedia* and *Endiandra* are the largest genera within this clade. The former includes ca. 250 species widely distributed across tropical regions of Africa, the Americas, Asia, and Oceania (Nishida, 1999; van der Werff, 2001), and the latter includes more than 100 species distributed from subtropical East Asia to Oceania (Arifiani, 2001; van der Werff, 2001). The remaining genera are small and have much more restricted distributions. *Sinopora* and *Hexapora* are monotypic and endemic to Hong Kong (Li et al., 2008b) and peninsular Malaysia, respectively (Kochummen, 1989; van der Werff, 2001; de Kok, 2016). *Yasunia* includes only two species distributed in tropical America (van der Werff and Nishida, 2010). *Syndiclis* includes ca. 10 species mainly distributed in southern China with one species in Bhutan (Li et al., 2008a). *Potameia* is endemic to Madagascar and includes ca. 20 species (van der Werff, 1991). It remains unclear how these genera are related and thus how to delimit them taxonomically (van der Werff and Nishida, 2010; Yang et al., 2012).

Early molecular phylogenetic investigations indicated that *Endiandra* and *Potameia* were nested within *Beilschmiedia* (Chanderbali et al., 2001; Rohwer and Rudolph, 2005). The updated phylogeny by Liu et al. (2013) demonstrated that *Syndiclis*, *Endiandra*, and *Beilschmiedia* were all monophyletic but their sampling was geographically restricted to Asia. Rohwer et al. (2014) subsequently inferred a phylogeny using two markers (nrITS and chloroplast *trn*K) with expanded species sampling. Their results supported the monophyly of *Yasunia* and *Endiandra*, and identified *Beilschmiedia* as paraphyletic. Their study also suggested that *Triadodaphne* should be incorporated into *Endiandra* because *Triadodaphne* was nested within *Endiandra*. In total, Rohwer et al. (2014) identified 11 well-supported clades [Posterior Probability (PP) greater than 0.95]. Relationships among many of the deeper nodes involving these clades, however, were mostly unresolved.

Syndiclis represents a key genus in the *Beilschmiedia* group because it displays huge variation in floral characteristics, including merosity, stamen number, and anther locule number (Zeng et al., 2017). Additionally, variation in features associated with this genus overlaps with that of other genera in the group, thus complicating our understanding of intergenic relationships (Hooker, 1886; Rohwer, 1993; van der Werff and Nishida, 2010; Zeng et al., 2017). As a result, this taxon has been a source of long-standing debate. It has even previously been treated as a synonym of *Potameia* (Kostermans, 1957; Li and Pai, 1982; Rohwer, 1993). Despite the great interest in this group, however, its phylogenetic placement remains unknown.

The above-mentioned systematic problems can be resolved with a robust phylogeny that applies appropriate taxon sampling and genetic markers with known ability to resolve challenging clades. Chloroplast genomes (plastomes) are a rich source of phylogenetic information, and are widely applied in phylogenetic studies for a number of reasons, e.g., uniparental inheritance and structural conservation, ease of sequencing, low recombination rates, conserved rates of nucleotide substitution, and the presence of abundant existing data (Zhang and Li, 2011; Gitzendanner et al., 2018). The plastome is applicable for inferring angiosperm relationships at varying phylogenetic depths. For example, slower evolving genes can be applied at deep phylogenetic scales while faster evolving genes and spacer regions are applicable at shallower depths (Gitzendanner et al., 2018). Moreover, the plastome has been shown to be especially valuable for resolving systematic problems in Lauraceae (Chen et al., 2017; Song et al., 2016, 2017a, 2017b; Li et al., 2017; Liao et al., 2018; Zhao et al., 2018).

Here, we applied Illumina HiSeq High Throughput technology to sequence plastomes representing 25 species spanning five genera and including most major clades identified by Rohwer et al. (2014) and Liu et al. (2013). We characterized macrostructural variation of these plastomes across the *Beilschmiedia* group, inferred their phylogeny using Maximum Likelihood and Bayesian Inference, and estimated their divergence times. Our results resolve several long-standing taxonomic debates, and illuminated our understanding of their diversification history.

Table 2
Plastome sequences obtained from NCBI and LCGDB for this study.

Species	Accession	Database
Actinodaphne cupularis (Hemsl.) Gamble	LAU00034	LCGDB
Actinodaphne lancifolia (Blume) Meisn.	MG581436	NCBI
Actinodaphne pilosa (Lour.) Merr.	LAU00035	LCGDB
Actinodaphne trichocarpa C.K. Allen	MF939342	NCBI
Alseodaphne gracilis Kosterm.	MG407593	NCBI
Alseodaphne hainanensis Merr. [=*Alseodaphnopsis hainanensis* (Merr.) H.W.Li & J.Li]	LAU00036	LCGDB
Alseodaphne huanglianshanensis H.W. Li & Y.M. Shui	MG407594	NCBI
Alseodaphne rugosa Merr. & Chun [=*Alseodaphnopsis rugosa* (Merr. & Chun) H.W.Li & J.Li]	LAU00037	LCGDB
Alseodaphne semecarpifolia Nees	MG407595	NCBI
Alseodaphne yunnanensis Kosterm.	LAU00038	LCGDB
Beilschmiedia pauciflora H.W.Li	MF939347	NCBI
Beilschmiedia robusta C.K. Allen	LAU00041	LCGDB
Beilschmiedia tungfangensis S.K. Lee & L.F. Lau	MF939348	NCBI
Beilschmiedia turbinata Bing Liu & Y. Yang	LAU00039	LCGDB
Calycanthus chinensis (W.C. Cheng & S.Y. Chang) P.T. Li	MG561304	NCBI
Calycanthus floridus var. *glaucus* (Willd.) Torr. & A. Gray	NC004993	NCBI
Caryodaphnopsis henryi Airy Shaw	MF939346	NCBI
Caryodaphnopsis malipoensis Bing Liu & Y. Yang	MF939343	NCBI
Caryodaphnopsis tonkinensis (Lecomte) Airy Shaw	LAU00043	LCGDB
Cassytha capillaris Meisn.	MF939338	NCBI
Cassytha filiformis L.	LC210517	NCBI
Chimonanthus nitens Oliv.	MH377058	NCBI
Chimonanthus praecox (L.) Link	MH377057	NCBI
Cinnamomum bodinieri H. Lév.	MH394418	NCBI
Cinnamomum burmanni (Nees & T. Nees) Blume	LAU00046	LCGDB
Cinnamomum camphora (L.) J. Presl	LC228240	NCBI
Cinnamomum cassia (L.) J. Presl [=*Cinnamomum aromaticum* Nees]	Under review	NCBI
Cinnamomum heyneanum Nees	LAU00047	LCGDB
Cinnamomum micranthum (Hayata) Hayata	KT833081	NCBI
Cinnamomum micranthum f. *kanehirae* (Hayata) S.S. Ying	KR014245	NCBI
Cinnamomum oliveri F.M. Bailey	KT716496	NCBI
Cinnamomum porrectum (Roxb.) Kosterm. [=*Cinnamomum parthenoxylon* (Jack) Meisn.]	MH050971	NCBI
Cinnamomum verum J. Presl	KY635878	NCBI
Cinnamomum yabunikkei H. Ohba	NC044864	NCBI
Cryptocarya chinensis (Hance) Hemsl.	LC212965	NCBI
Cryptocarya hainanensis Merr.	MF939350	NCBI
Dehaasia incrassata (Jack) Kosterm.	LAU00052	LCGDB
Endiandra discolor Benth.	KT588615	NCBI
Endiandra dolichocarpa S.K. Lee & Y.T. Wei	LAU00053	LCGDB
Endiandra globosa Maiden & Betche	KT588614	NCBI
Endiandra muelleri Meisn.	LAU00054	LCGDB
Eusideroxylon zwageri Teijsm. & Binn.	MF939351	NCBI
Gyrocarpus americanus Jacq.	ERR2040128	NCBI
Idiospermum australiense (Diels) S.T. Blake	MH377056	NCBI
Illigera celebica Miq.	Under review	NCBI
Illigera grandiflora W.W. Sm. & Jeffrey	Under review	NCBI
Iteadaphne caudata (Nees) H.W. Li	LAU00055	LCGDB
Laurus azorica (Seub.) Franco	MK041220	NCBI
Laurus nobilis L.	LAU00056	LCGDB
Lindera aggregata (Sims) Kosterm.	MG581437	NCBI
Lindera angustifolia W.C. Cheng	MG581438	NCBI
Lindera benzoin (L.) Blume	MH220730	NCBI
Lindera chunii Merr.	MG581439	NCBI
Lindera communis Hemsl.	MH220731	NCBI
Lindera erythrocarpa Makino	MG581441	NCBI
Lindera floribunda (C.K. Allen) H.B. Cui	MG581442	NCBI
Lindera fragrans Oliv.	MN453265	NCBI
Lindera glauca (Siebold & Zucc.) Blume	MF188124	NCBI
Lindera latifolia Hook. f.	MH220733	NCBI
Lindera limprichtii H. Winkl.	MN453266	NCBI
Lindera megaphylla Hemsl.	MH220734	NCBI
Lindera metcalfiana C.K. Allen	MH220735	NCBI
Lindera nacusua (D. Don) Merr.	MH220736	NCBI
Lindera neesiana (Wall. ex Nees) Kurz	MG581447	NCBI
Lindera obtusiloba Blume	MH220737	NCBI
Lindera praecox (Siebold & Zucc.) Blume	MG581449	NCBI
Lindera pulcherrima (Nees) Hook. f.	LAU00082	LCGDB
Lindera reflexa Hemsl.	MG581451	NCBI
Lindera robusta (C.K. Allen) H.B. Cui	MH220738	NCBI
Lindera rubronervia Gamble	MG581452	NCBI
Lindera sericea (Siebold & Zucc.) Blume	MG581453	NCBI
Lindera supracostata Lecomte	MN453269	NCBI
Lindera thomsonii C.K. Allen	MN453272	NCBI
Litsea cubeba (Lour.) Pers.	LAU00060	LCGDB
Litsea glutinosa (Lour.) C.B. Rob.	KU382356	NCBI
Litsea japonica (Thunb.) Juss.	MG581454	NCBI
Litsea magnoliifolia Yang & P.H. Huang	LAU00062	LCGDB
Litsea monopetala (Roxb.) Pers.	LAU00063	LCGDB
Litsea panamanja (Buch.-Ham. ex Nees) Hook. f.	LAU00064	LCGDB
Litsea pierrei Lecomte	LAU00065	LCGDB
Litsea tsinlingensis Yang & P.H. Huang	LAU00059	LCGDB
Machilus balansae (Airy Shaw) F.N. Wei & S.C. Tang	KT348517	NCBI
Machilus fasciculata H.W. Li	LAU00066	LCGDB
Machilus minutiloba S.K. Lee	LAU00069	LCGDB
Machilus pauhoi Kaneh.	MH178403	NCBI
Machilus thunbergii Siebold & Zucc.	MH178404	NCBI
Machilus yunnanensis Lecomte	KT348516	NCBI
Nectandra angustifolia (Schrad.) Nees & Mart.	MF939340	NCBI
Neocinnamomum caudatum (Nees) Merr.	MF939344	NCBI
Neocinnamomum delavayi (Lecomte) H. Liu	LC213014	NCBI
Neocinnamomum lecomtei H. Liu	MF939345	NCBI
Neocinnamomum mekongense (Hand.-Mazz.) Kosterm.	MF686120	NCBI
Neolitsea chui Merr.	LAU00070	LCGDB
Neolitsea oblongifolia Merr. & Chun	LAU00071	LCGDB
Neolitsea sericea (Blume) Koidz.	MF939341	NCBI
Nothaphoebe umbelliflora (Blume) Blume	LAU00072	LCGDB
Parasassafras confertiflorum (Meisn.) D.G. Long	MH729378	NCBI
Persea americana Mill.	KX437771	NCBI
Persea americana var. *americana*	MK959366	NCBI
Persea americana var. *drymifolia* (Schltdl. & Cham.) S.F. Blake	LAU00073	LCGDB
Persea borbonia (L.) Spreng.	MK959370	NCBI
Peumus boldus Molina	ERR2040134	NCBI
Phoebe bournei (Hemsl.) Yang	MF315088	NCBI
Phoebe chekiangensis P.T. Li	KY346511	NCBI
Phoebe lanceolata (Wall. ex Nees) Nees	LAU00075	LCGDB
Phoebe neurantha (Hemsl.) Gamble	MH394352	NCBI
Phoebe omeiensis R.H. Miao	NC031190	NCBI
Phoebe sheareri (Hemsl.) Gamble	KX437773	NCBI
Phoebe zhennan S.K. Lee & F.N. Wei	MH033832	NCBI
Sassafras tzumu (Hemsl.) Hemsl.	MG581455	NCBI
Syndiclis anlungensis H.W. Li	LAU00076	LCGDB
Syndiclis marlipoensis H.W. Li	LAU00077	LCGDB
Wilkiea hugeliana (Tul.) A. DC.	KT716505	NCBI

Note: LCGDB = Lauraceae Chloroplast Genome Database. Sequences from LCGDB and NCBI under review were provided by Y. Song.

2. Materials and methods

2.1. Taxon sampling

Twenty-five species belonging to five genera of the *Beilschmiedia* group were newly sampled for our study (Table 1). Fresh leaves were dried with silica gel in the field. We also included 10 previously published plastomes of the *Beilschmiedia* group (Table 2). Our sampling was guided by previous investigations by Liu et al. (2013) and Rohwer et al. (2014). In particular, we sampled eight representatives of the 11 major clades identified by Rohwer et al. (2014). Our sampling also covered the broad geographic range of the clade, including representatives from Africa, Madagascar, Asia, Australasia, and the Americas. We were unsuccessful in our efforts to extract DNA from *Yasunia sessiflora* van der Werff, and thus unable to include a representative of this South American group. In addition, we did not include the monotypic *Hexapora*, which has not been collected for over 100 years (de Kok, 2016). Finally, biogeographic representation was sparse across key areas, especially in the neotropics, southeastern Asia, and Africa.

To estimate molecular divergence times of the *Beilschimedia* group,

we expanded our sampling more broadly across Lauraceae to ensure sufficient representation for assigning appropriate fossil calibrations (Table 2; and see below for fossil calibrations). This included 103 previously published plastomes representing 22 genera of the family Lauraceae, plus seven genera representing four additional non-Lauraceae families of Laurales. Phylogenetic investigations have indicated that Calycanthaceae are sister to all Laurales (Renner, 2004; Song et al., 2019), and were thus designated as outgroup.

2.2. DNA extraction and genomic sequencing

Total genomic DNA was extracted using the plant genomic extraction kit BIOBETTER (GeneBetter Biotech Co., Ltd, Beijing, China). DNA quality was assessed with agarose gel electrophoresis and a NanoDrop-2000 spectrometer (Thermo Scientific, U.S.A.). The total DNA of each sample was randomly fragmented to generate a short-insert library (length ~400 bp). Genomic libraries were sequenced using an Illumina HiSeq 4000 platform (Majorbio, Beijing, China). A total of ~3 Gb of 150 bp paired-end reads were obtained for each sample.

2.3. Genome assembly and annotation

Raw reads were filtered using Fastp (https://github.com/OpenGene/fastp) to remove low-quality reads. Filtered reads were assembled into contigs using SPAdes v3.10.1 (Bankevich et al., 2012). Kmer length was set to 95. The plastome contigs were filtered using a local screening Blast. A previously published chloroplast genome of *B. tungfangensis* S.K. Lee & L.F. Lau (Accession No. MF939348) was selected as a reference for assembly. The IRa region of this reference was deleted; contigs plus the reference genome were then loaded into Sequencher 5.4.5 (Gene Codes Corp., Ann Arbor, Michigan, USA); contigs with low coverage (< 50) were removed at this time. All contigs were assembled against the reference genome; cleaned reads and the assembled sequence were next loaded in Geneious 10.0.2 (Kearse et al., 2012). Cleaned reads were remapped against our reference-guided assembly and proofed for accuracy. The remapped reads were manually curated to correct errors and assembly ambiguities. Boundaries of the large single copy (LSC), small single copy (SSC), and inverted repeat (IR) regions were detected using BLAST (https://www.ncbi.nlm.nih.gov/). The final plastome assemblies were annotated using Plann 1.1 (Huang and Cronk, 2015). Assembled plastomes were loaded into Sequin (https://www.ncbi.nlm.nih.gov/Sequin/index.html), and genes that remained unannotated or erroneously annotated were manually deleted or edited. All annotated plastomes were deposited in GenBank (Table 1). Circular genome maps were drawn using the OrgallellarGenomeDRAW software (OGDRAW, Lohse et al., 2013).

2.4. Repeat sequence analyses

The software REPuter (https://bibiserv.cebitec.uni-bielefeld.de/reputer/, Kurtz et al., 2001) was used to identify repeat sequences including forward, reverse, complement, and palindromic sequences according to the following parameters: 1) hamming distance of 3, 2) sequence identity ≥ 90%, and 3) minimum repeat size ≥ 20 bp. MISA (MIcroSAtellite identification tool, http://pgrc.ipk-gatersleben.de/misa/) was implemented to identify short sequence repeats (SSRs) in the chloroplast genomes with the parameters set to ten for mononucleotides, five for dinucleotides, four for trinucleotides, and three for tetranucleotide, pentanucleotide, and hexanucleotide SSRs.

2.5. Macrostructural plastome analysis

To more fully characterize the chloroplast genomes of the *Beilschmiedia* group, we conducted a macrostructural analysis of these genomes. To accomplish this, complete chloroplast genomes were aligned with MAFFT 7.2 (Katoh and Standley, 2013), and manually adjusted. A sliding window analysis using DnaSP 6.0 was conducted to compute nucleotide diversity (Pi value, Rozas et al., 2017). Sliding window length was set to 600 bp and the step size to 200 bp. We also used the Shuffle-LAGAN model in mVISTA (http://genome.lbl.gov/vista/mvista/submit.shtml) to analyze the genome differences among genera of the *Beilschmiedia* group.

2.6. Phylogenetic inference

Protein-coding sequences, RNA-coding sequences, and non-coding sequences were extracted using Geneious ver. 10.0.2 (Kearse et al., 2012). These sequences were aligned in MAFFT ver. 7.2. We assembled three data matrices and inferred a phylogeny for each: coding sequences only (datamatrix I), non-coding sequences only (datamatrix II), and all concatenated data (datamatrix III). The appropriate nucleotide substitution models were determined using MrModeltest 2.3 (Nylander, 2004) based on the Akaike information criterion (AIC; Akaike, 1973). We inferred phylogenetic trees using Maximum likelihood (ML) and Bayesian inference (BI) methods. To infer ML trees, RAxML-HPC2 7.6.3 as implemented in CIPRES (http://www.phylo.org/) was performed; one thousand bootstrap replicates were performed in each analysis to assess confidence. To infer BI trees, MrBayes 3.2.6 was implemented on XSEDE in CIPRES (http://www.phylo.org/). Markov Chain Monte Carlo (MCMC) chains were run for 1,000,000 generations, and trees were sampled every 1000 generations. The first 25% of trees from all runs were discarded as burnin.

2.7. Molecular divergence time estimation

We employed BEAST v. 2.3.0 (Drummond et al., 2012) to estimate divergence times with a Yule process for the tree prior model and a relaxed clock using the log normal distribution. We used BEAUti v.2.3.0 to create an input file for running BEAST. The nucleotide substitution model was designated as GTR. Three independent MCMC chains were run for 80,000,000 generations (burnin 10%), and were sampled every 8,000 generations. The log and tree files of the three runs were combined using LogCombiner (Drummond et al., 2012). We then used Tracer v. 1.5 (http://tree.bio.ed.ac.uk/software/tracer) to check the combined log file to ensure that all values of the effective sample size (ESS) were greater than 200 and that plots of the three analyses converged accordingly. The combined tree was annotated with TreeAnnotator v. 2.3.0 (Drummond et al., 2012). The resulting tree was visualized using FigTree v. 1.4.0 (Rambaut, 2009).

2.8. Fossil calibrations

We applied six macrofossils to calibrate our phylogenetic tree for divergence time estimation (Table 3). First, *Virginianthus calycanthoides* Friis et al. is a middle Albian fossil nested within the Laurales, either assigned to Calycanthaceae (Friis et al., 1994), or as sister to Calycanthaceae or the remaining Laurales (Doyle et al., 2008; Doyle and Endress, 2010). We applied this fossil to calibrate the crown age of Laurales [C1: age 107.7 million years ago (Ma)] following Massoni et al. (2015). For this node, we set a log normal prior distribution with an offset of 107.1 Ma, a mean of 0.5, and a standard deviation of 0.6. Second, the charcoalified flower *Potomacanthus lobatus* von Balthazar et al. possesses typical floral characters of Lauraceae, e.g., bisexual and trimerous, tepals in two whorls, fertile stamens in two whorls, valvate anthers, and gynoecium consisting of a single carpel containing a single ovule (von Balthazar et al., 2007). We followed Kondraskov et al. (2015) and applied this fossil to calibrate the stem node of Lauraceae (C2: age 106.8 Ma, Kondraskov et al., 2015). Here, we assigned a log normal prior distribution with an offset of 106.8 Ma, a mean of 0.5, and a standard deviation of 0.6. Third, *Jerseyanthus calycanthoides* Crepet et al. is from the Raritan Formation of New Jersey, U.S.A. The age of this fossil is believed to be in the Late Cretaceous, ca. 85.8 Ma (Massoni

Table 3
Fossil calibration of dating analyses of Lauraceae.

Node	Calibration fossil	Minimum Age (Ma)	Prior distribution	Prior parameters	2.5/median/97.5% quantiles (Ma)	Fossil References
C1: crown node of Laurales	*Virgianthus calycanthoides* Friis et al.	107.7	log normal	offset:107.1; M:0.5; SD:0.6	108/108/109	von Balthazar et al. (2011)
C2: stem node of Lauraceae	*Potomacanthus lobatus* von Balthazar et al.	106.8	log normal	offset:106.8; M:0.5; SD:0.6	107/107/108	von Balthazar et al. (2007); Kondraskov et al. (2015)
C3: divergence between *Chimonanthus* Lindl. and *Calycanthus* L.	*Jerseyanthus calycanthoides* Crepet et al.	85.8	log normal	offset:85.8; M:0.5; SD:0.6	85.9/86.2/87.2	Massoni et al. (2015)
C4: stem node of *Neocinnamomum* H. Liu	*Neusenia tetrasporangiata* Eklund	83.6	log normal	offset:83.6; M:0.5; SD:0.6	83.7/84/85	Eklund (2000)
C5: crown node of the *Persea* group	*Alseodaphne changchangensis* Jin & Li	43	log normal	offset:43; M:0.5; SD:0.6	43.1/43.4/44.4	Li et al. (2009)
C6: stem node of *Machilus* Nees	*Machilus maomingensis* Tang et al.	33.7	log normal	offset:33.7; M:0.5; SD:0.5	33.9/34.1/34.9	Li et al. (2016a); Tang et al. (2016)

M: mean; SD: standard deviation.

et al., 2015). A phylogenetic study of the Calycanthaceae including fossil species has suggested that *Jerseyanthus* Crepet et al. is sister to *Calycanthus* L. (Crepet et al., 2005). We thus used this to calibrate the split between *Calycanthus* and *Chimonanthus* Lindl. (C3: age 85.8 Ma) by setting a log normal prior distribution, an offset of 85.8 Ma, a mean of 0.5, and a standard deviation of 0.6. Fourth, the Cretaceous fossil taxon *Neusenia tetrasporangiata* Eklund has been hypothesized to be related to *Neocinnamomum* H. Liu owing to its psilate pollen grains (Eklund, 2000; Atkinson et al., 2015). We thus used it to calibrate the stem age of *Neocinnamomum* (C4: age 83.6 Ma) by setting a log normal prior distribution with an offset of 83.6 Ma, a mean of 0.5, and a standard deviation of 0.6. Fifth, *Alseodaphne changchangensis* Jin & Li is a fossil species from the Changchang Formation of Hainan, China (Li et al., 2009). The age of this fossil is dated to late Early Eocene to early Late Eocene (Li et al., 2011). We followed Li et al. (2011) and applied this fossil to calibrate the crown age of the *Persea* group (C5: age 37–48 Ma). We assigned a log normal prior distribution with an offset of 43 Ma, a mean of 0.5, and a standard deviation of 0.6. Sixth, *Machilus maomingensis* Tang et al. is a fossil species from the Youganwo Formation of Guangdong, China (Tang et al., 2016). The locality of this fossil is dated to the Eocene–Oligocene boundary (ca. 33.7–33.9 Ma, Li et al., 2016a). The age of *Machilus* Nees is dated to Early Miocene ca. 20 Ma (Li et al., 2011). We therefore applied a minimum age to calibrate the stem age of *Machilus* (C6: age 33.7 Ma) by setting a log normal prior distribution with an offset of 33.7 Ma, a mean of 0.5, and a standard deviation of 0.5.

3. Results

3.1. DNA extraction, genomic sequencing, and assembly

A total 25 plastomes from an equal number of species were newly sequenced from the *Beilschmiedia* group. Details of sequencing and assemblies were summarized in Table S1.

3.2. Characteristics of chloroplast genomes of the Beilschmiedia group

All species possessed the canonical quadripartite plastome structure (Fig. 1). All plastomes contained a pair of inverted repeat (IRs) regions, which separated the large and small single copy regions, respectively (LSC and SSC, respectively). Variation in genome size was very small between species and ranged from 157,423 bp in the Australian *B. tooram* (Bailey) B. Hyland to 158,671 bp in the American *B. brenesii* C.K. Allen (Table 4). The size of the LSC ranged from 88,407 bp in *B. tooram* to 89,600 bp in *B. brenesii*. The size of the SSC ranged from 18,008 bp in *B. tooram* to 18,383 bp in *B. brunnea* B. Hyland. IRs ranged from 25,315 bp in *B. brunnea* to 25,581 bp in *P. microphylla* Kosterm. The GC content of the plastomes was 39% on average, and exhibited little variation between species. The IR regions contained more G and C than the LSC and SSC regions; the GC content was 43% in the IR regions, and 37% and 34% in the LSC and SSC regions, respectively.

A total of 131 genes were annotated for each species for the newly assembled genomes. We identified 86 protein-coding genes, 37 tRNA genes, and eight rRNA genes for each genome (Table 5). Among these 131 genes, 18 were found to possess introns, including 12 protein-coding genes, i.e., *clpP*, *ycf3*, *atpF*, *ndhA*, *ndhB*, *petB*, *petD*, *rpl2*, *rpl16*, *rpoC1*, *rps12*, and *rps16*, and six tRNA genes, i.e. *trnA-UGC*, *trnG-UCC*, *trnI-GAU*, *trnK-UUU*, *trnL-UAA*, and *trnV-UA*. Among these 18 genes, only *clp*P and *ycf*3 contained two introns while the other 16 genes possessed only one intron in each of them. The gene *rps12* was a *trans*-spliced gene with the 5′ end located in the LSC region and the duplicated 3′ end in the IR region.

3.3. Repeat structure and simple sequence repeats

We detected 89 repeats on average for each species we sampled

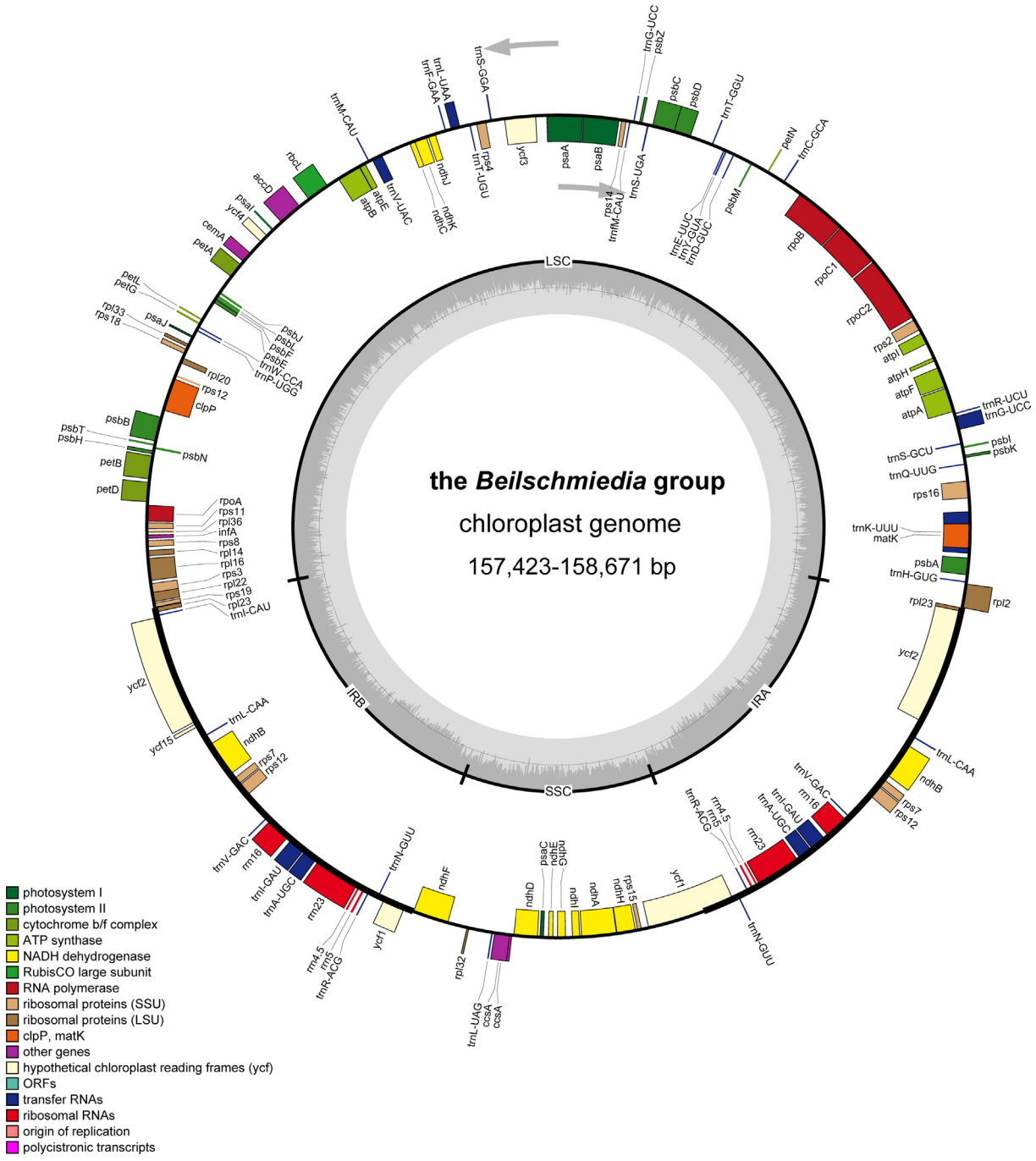

Fig. 1. Circular gene map of the *Beilschmiedia* group including 25 species. Genes drawn outside the circle are transcribed in the counterclockwise direction, those inside are transcribed in the clockwise direction. Different colored bars represent genes with different functions. The dashed dark gray area in the inner circle indicates the GC content of the plastome, and the light gray area shows the AT content.

(Fig. S1). These repeats included forward, reverse, complement, and palindromic repeats; the palindromic repeats had the highest proportion (ca. 40%), followed by the forward repeats (ca. 32%), the reverse repeats (ca. 21%), and the complement repeats (ca. 7%). The repeats mostly ranged from 20 to 40 bp; the longest repeat was 81 bp of the forward repeat and the complement repeat, which was found in *P. microphylla*.

Simple sequence repeats (SSRs) were detected in all species (Fig. S2). Our MISA analysis identified SSRs ranging from 106 in *E. monothyra* B. Hyland subsp. *monothyra* to 127 in *B. brachythyrsa* H.W. Li and *B. glauca* S.K. Lee & L.F. Lau. Mononucleotide repeats were the most common SSRs, as many as 105 were found in *B. brenesii*, *B. brachythyrsa*, and *B. glauca* while only 80 were identified in *E. monothyra* subsp. *monothyra* (Fig. S2). Hexanucleotide repeats were only found in eight species including *B. pierreana* Robyns & R. Wilczek, *B. obtusifolia* (Meisn.) F. Muell., *Syndiclis* sp., *E. monothyra* subsp. *monothyra*, *E. xanthocarpa* B. Hyland, *E. montana* C.T. White, *E. microneura* C. White, and *P. microphylla* (Fig. S3).

3.4. Sequence divergence

The sampled plastomes showed high similarity and low divergence within the *Beilschmiedia* group. The Pi values within 600 bp across the 25 plastomes ranged between 0 and 0.0193 and the mean value was

Table 4
A comparison of the 25 plastomes of the *Beilschmiedia* group.

Characteristics	*B. appendiculata*	*B. brachythyrsa*	*B. brunnea*	*B. brenesii*	*B. brevipaniculata*	*B. delicata*	*B. fasciata*	*B. glauca*
Total cpDNA size (bp)	158,639	158,546	158,323	158,671	158,475	158,518	158,414	158,566
Length of large single copy (LSC) region (bp)	89,426	89,388	89,312	89,600	89,339	89,328	89,295	89,381
Length of small single copy (SSC) region (bp)	18,227	18,162	18,383	18,143	18,196	18,222	18,205	18,177
Length of inverted repeat (IRs) region (bp)	25,493	25,498	25,314	25,464	25,470	25,484	25,457	25,504
Total GC content (%)	38.98%	39.01%	39.02%	39.98%	39.00%	39.00%	39.01%	38.96%
LSC-GC content (%)	37.69%	37.75%	37.77%	37.68%	37.73%	37.74%	37.74%	37.68%
SSC-GC content (%)	33.97%	33.97%	33.93%	33.95%	33.97%	33.93%	34.01%	33.87%
IR-GC content (%)	43.03%	43.01%	43.07%	43.07%	43.02%	43.02%	43.03%	43.03%
Total number of genes	131	131	131	131	131	131	131	131
Total number of protein encoding genes	86	86	86	86	86	86	86	86
Total number of tRNA genes	37	37	37	37	37	37	37	37
Total number of rRNA genes	8	8	8	8	8	8	8	8

Characteristics	*B. immersinervis*	*B. obtusifolia*	*B. pergamentacea*	*B. pierreana*	*B. rufohirtella*	*B. purpurascens*	*B. tooram*	*B. yunnanensis*
Total cpDNA size (bp)	158,564	158,233	158,438	158,553	158,496	158,416	157,423	158,443
Length of large single copy (LSC) region (bp)	89,351	89,036	89,280	89,298	89,315	89,314	88,407	89,259
Length of small single copy (SSC) region (bp)	18,235	18,205	18,182	18,291	18,211	18,178	18,008	18,228
Length of inverted repeat (IRs) region (bp)	25,489	25,496	25,488	25,482	25,485	25,462	25,504	25,478
Total GC content (%)	39.00%	39.09%	38.99%	39.00%	38.98%	38.99%	39.09%	38.96%
LSC-GC content (%)	37.75%	37.85%	37.71%	37.75%	37.71%	37.72%	37.85%	37.71%
SSC-GC content (%)	33.86%	34.01%	33.93%	33.85%	33.91%	33.98%	34.00%	33.35%
IR-GC content (%)	43.05%	43.06%	43.04%	43.05%	43.03%	43.01%	43.04%	43.04%
Total number of genes	131	131	131	131	131	131	131	131
Total number of protein encoding genes	86	86	86	86	86	86	86	86
Total number of tRNA genes	37	37	37	37	37	37	37	37
Total number of rRNA genes	8	8	8	8	8	8	8	8

Characteristics	*E. microneura*	*E. monothyra* subsp. *monothyra*	*E. montana*	*E. xanthocarpa*	*P. microphylla*	*S. fooningensis*	*S. hongkongensis*	*S. kwangsiensis*	*S.* sp
Total cpDNA size (bp)	158,598	158,552	158,645	158,431	158,597	158,576	158,598	158,654	158,640
Length of large single copy (LSC) region (bp)	89,330	89,285	89,363	89,166	89,245	89,386	89,391	89,455	89,409
Length of small single copy (SSC) region (bp)	18,232	18,229	18,242	18,235	18,142	18,200	18,205	18,205	18,119
Length of inverted repeat (IRs) region (bp)	25,518	25,519	25,520	25,515	25,605	25,495	25,501	25,497	25,556
Total GC content (%)	39.05%	39.05%	39.03%	39.03%	39.03%	39.01%	39.01%	39.01%	39.01%
LSC-GC content (%)	37.80%	37.81%	37.78%	37.78%	37.79%	37.74%	37.75%	37.73%	37.74%
SSC-GC content (%)	34.04%	34.00%	33.99%	33.88%	34.03%	33.93%	33.95%	33.96%	33.99%
IR-GC content (%)	43.04%	43.05%	43.03%	43.04%	42.97%	43.05%	43.03%	43.04%	43.02%
Total number of genes	131	131	131	131	131	131	131	131	131
Total number of protein encoding genes	86	86	86	86	86	86	86	86	86
Total number of tRNA genes	37	37	37	37	37	37	37	37	37
Total number of rRNA genes	8	8	8	8	8	8	8	8	8

Table 5
Annotated genes of the 25 plastomes of the *Beilschmiedia* group.

Category of genes	Group of genes	Names of genes
Transcription- and translation-related genes	Ribosomal proteins	*rps2*, *rps3*, *rps4*, *rps7*$^{(\times 2)}$, *rps8*, *rps11*, *rps12*$^{*(\times 2)}$, *rps14*, *rps15*, *rps16**, *rps18*, *rps19* *rpl2**, *rpl14*, *rpl16**, *rpl20*, *rpl22*, *rpl23*$^{(\times 2)}$, *rpl32*, *rpl33*, *rpl36*
	Transcription	*rpoA*, *rpoB*, *rpoC1**, *rpoC2*
	Translation initiation factor	*infA*
RNA genes	Transfer RNA	*trnA-UGC*$^{*(\times 2)}$, *trnC-GCA*, *trnD-GUC*, *trnE-UUC*, *trnF-GAA*, *trnfM-CAU*, *trnG-UCC*$^{*(\times 2)}$, *trnH-GUG*, *trnI-CAU*, *trnI-GAU*$^{*(\times 2)}$, *trnK-UUU**, *trnL-CAA*$^{(\times 2)}$, *trnL-UAA**, *trnL-UAG*, *trnM-CAU*$^{(\times 2)}$, *trnN-GUU*$^{(\times 2)}$, *trnP-UGG*, *trnQ-UUG*, *trnR-ACG*$^{(\times 2)}$, *trnR-UCU*, *trnS-GCU*, *trnS-GGA*, *trnS-UGA*, *trnT-GGU*, *trnT-UGU*, *trnV-GAC*$^{(\times 2)}$, *trnV-UAC**, *trnW-CCA*, *trnY-GUA*
	Ribosomal RNA	*rrn4.5*$^{(\times 2)}$, *rrn5*$^{(\times 2)}$, *rrn16*$^{(\times 2)}$, *rrn23*$^{(\times 2)}$
Photosynthesis-related genes	Photosystem I	*psaA*, *psaB*, *psaC*, *psaI*, *psaJ*
	Photosystem II	*psbA*, *psbB*, *psbC*, *psbD*, *psbE*, *psbF*, *psbH*, *psbI*, *psbJ*, *psbK*, *psbL*, *psbM*, *psbN*, *psbT*, *lhbA*
	ATP synthase	*atpA*, *atpB*, *atpE*, *atpF**, *atpH*, *atpI*
	Cytochrome *b*/f complex	*petA*, *petB**, *petD**, *petG*, *petL*, *petN*
	Assembly and stability of photosystem I	*ycf3***, *ycf4*
	NADPH dehydrogenase	*ndhA**, *ndhB*$^{*(\times 2)}$, *ndhC*, *ndhD*, *ndhE*, *ndhF*, *ndhG*, *ndhH*, *ndhI*, *ndhJ*, *ndhK*
	Rubisco	*rbcL*
	Cytochrome *c* synthesis	*ccsA*
Miscellaneous group	Maturase	*matK*
	Acetyl-CoA carboxylase	*accD*
	Cytochrome	
	Inner membrane protein	*cemA*
	ATP-dependent protease Inner	*clpP***
	conserved reading frames	*ycf1*$^{(\times 2)}$, *ycf2*$^{(\times 2)}$
	Pseudogenes	*ycf15*

*Genes with one intron, **Genes with two introns, $^{(\times 2)}$duplicate genes.

0.003 (Fig. S4A). Three genes, i.e. *ycf*2, *ndh*F, and *rpl*32, had Pi values over 0.01 and showed markedly higher variability than other regions (Fig. S4A). Across Lauraceae, the Pi value varied between 0 and 0.07051 and the mean was 0.02, demonstrating higher variability than that within the *Beilschmiedia* group (Fig. S4B).

We conducted the mVISTA analysis with reference to *Cryptocarya chinensis* (Hance) Hemsl., and obtained gene loci of the 25 chloroplast genomes (Fig. S5). In general, non-coding regions possessed higher variation than coding regions, and IR regions were less divergent than SSC and LSC regions.

3.5. Phylogenetic analysis

Our sequence data for phylogeny consisted of 138 plastomes including 35 species of the *Beilschmiedia* group. The aligned data matrices, including coding, noncoding, and complete sequences, were 79,992, 66,634, and 159,819 bp in length, respectively. These regions contain 1,228, 1,461, and 2,748 bp parsimony informative sites, respectively. Nucleotide substitution model for the BI analysis is GTR + G + I.

ML and BI phylogenies inferred from the coding regions (datamatrix I) were the best resolved and not obviously in conflict with other analyses. These results are displayed here (Figs. 2, S6, S7), and discussed below. The monophyletic *Beilschmiedia* group contains two large clades, an Australasian clade and a second clade including species from Africa, Asia, and the Americas (Fig. 2). The Australasian clade is relatively well supported (PP: 1, BS: 99%), and contains three *Beilschmiedia* species and a monophyletic *Endiandra* (PP: 1, BS: 100%). *Endiandra globosa* Maiden & Betche and *E. xanthocarpa* form a small clade that is sister to the remaining *Endiandra* species. The Asian *E. dolichocarpa* S.K. Lee & Y.T. Wei is sister to a clade containing the Australasian *E. montana* (syn.: *Brassiodendron fragrans* C.K. Allen), *E. microneura*, *E. muelleri* Meisn., *E. monothyra* subsp. *monothyra* and *E. discolor* Benth. The second clade in the *Beilschmiedia* group includes an African subclade and a subclade containing species from Asia and America (PP: 1, BS: 100%). The African clade consists of the Malagasy *P. microphylla* and *B. pierreana* from Gabon in African mainland (PP: 1, BS: 100%). *Beilschmiedia immersinervis* Sachiko Nishida is sister to a subclade including all Asian species and one American species (PP: 1, BS: 100%). This subclade contains four lineages, i.e., Asian *B. turbinata* Bing Liu & Y. Yang, *B. glauca*, the *Sinopora* + *Syndiclis* subclade, and the American *B. brenesii* plus the large clade consisting of core Asian *Beilschmiedia* species. Relationships among these four lineages are unresolved. *Sinopora* and the Chinese *Syndiclis* form a well-supported clade (PP: 1, BS: 100%), but relationships within this clade are poorly resolved. A sister relationship between the American *B. brenesii* and the Asian *Beilschmiedia* clade received strong support (PP: 1, BS: 96%). The Asian *Beilschmiedia*, except *B. turbinata* and *B. glauca*, formed a robust clade with strong support (PP: 1, BS: 100%). Relationships within this Asian clade are also well resolved. The *Beilschmiedia* species group with small terminal buds is paraphyletic and contains four small subclades each consisting of a pair of species, i.e., *B. appendiculata* (C.K. Allen) S.K. Lee & Y.T. Wei and *B. pauciflora* H.W. Li (PP: 1, BS: 100%), *B. rufohirtella* H.W. Li and *B. pergamentacea* C.K. Allen (PP: 1, BS: 100%), *B. tungfangensis* and *B. yunnanensis* Hu (PP: 1, BS: 100%), and *B. delicata* S.K. Lee & Y.T. Wei and *B. brachythyrsa* (PP: 1, BS: 100%). The species group with large terminal buds constitutes a well-supported subclade and includes *B. robusta* C.K. Allen, *B. fasciata* H.W. Li, *B. purpurascens* H.W. Li, and *B. brevipaniculata* C.K. Allen (PP: 1, BS: 100%); this group is nested within the species group with small buds, and is in turn sister to a clade including *B. brachythyrsa* and *B. delicata* (PP: 1, BS: 99%).

3.6. Molecular divergence time estimation

Lauraceae diverged from Calycanthaceae in the Albian during the Early Cretaceous, ca. 108.5 Ma. The stem age of Lauraceae is during the Albian of the Early Cretaceous, ca. 107.3 Ma (Fig. S8). Divergence of the *Beilschmiedia* group from *Cryptocarya* R. Br. occurred in the Early Eocene, ca. 50.4 Ma (Fig. 3, node 1, Table 6). The age of the crown node of the *Beilschmiedia* group is inferred to have occurred by the latest Eocene, ca. 34.2 Ma (Fig. 3, node 2, Table 6). The crown age of the Australasian clade is in the Late Oligocene, ca. 27.2 Ma (Fig. 3, node 3, Table 6), and the split between *Endiandra* and the Australasian *Beilschmiedia* occurred at the Oligocene-Miocene boundary, ca. 22.3 Ma (Fig. 3). The crown age of *Endiandra* is ca. 11.9 Ma (Fig. 3, node 4, Table 6); the Asian *E. dolichocarpa* diverged from its Australasian

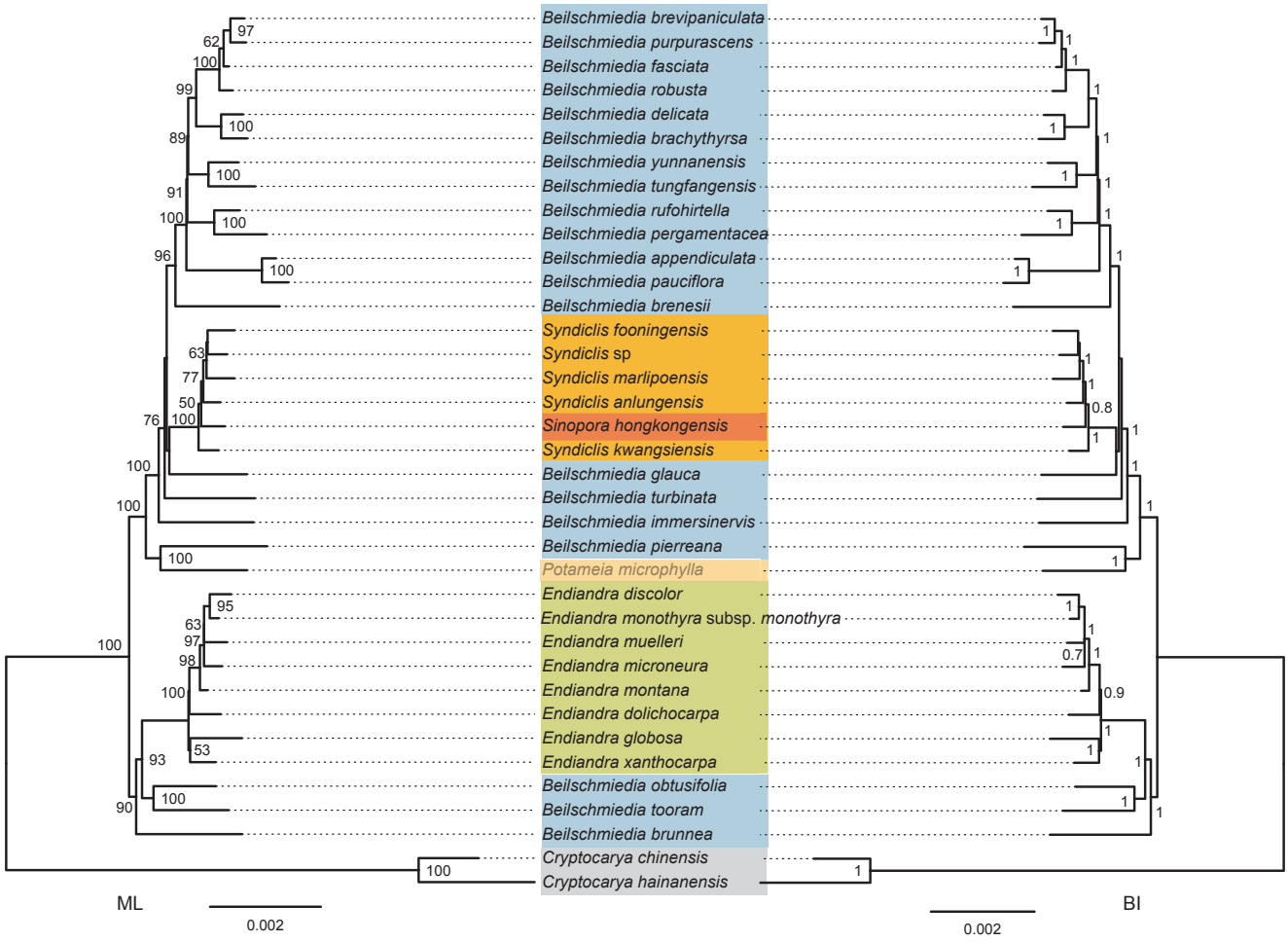

Fig. 2. Phylogeny of the *Beilschmiedia* group integrating ML and BI trees based on coding regions of plastomes. Numbers above at the nodes of ML tree (left) represent bootstrap percentages (BS, %) and those of BI tree (right) indicate Bayesian inference posterior probabilities (PP); BS and PP are displayed when they are greater than 50% and 0.7 respectively.

relatives ca. 10.5 Ma (Fig. 3, node 5, Table 6). The African clade diverged from the Asian and American species in the Early Oligocene, ca. 29.1 Ma (Fig. 3, node 6). Divergence between species from the African mainland and Madagascar, *Potameia microphylla* versus *B. pierreana,* respectively, occurred ca. 18.4 Ma (Fig. 3, node 7, Table 6). The American *B. immersinervis* diverged from the mainly Asian clade in the Late Oligocene, ca. 25.1 Ma (Fig. 3, node 8, Table 6), and the American *B. brenesii* diverged from the Asian core *Beilschmiedia* clade in the Early Miocene ca. 18.1 Ma (Fig. 3, node 9, Table 6). The crown age of *Sinopora* plus *Syndiclis* is in the Late Miocene 10.2 Ma (Fig. 3, node 10, Table 6).

4. Discussion

The robust phylogeny we inferred from 25 newly sampled plastomes greatly improves the phylogeny of the *Beilschmiedia* group and provides novel insights into the systematics and approximate divergence times of the group. We outline our results in the subsections below.

4.1. Backbone phylogeny of Beilschmiedia

Beilschmiedia is the largest genus in the *Beilschmiedia* group, and includes ca. 250 species widely distributed in pantropical regions. Rohwer et al. (2014) inferred a number of well-supported subclades within this group with strong geographical endemism, but relationships among these subclades were largely unresolved. Our study reconstructed a well-supported backbone phylogeny and laid a solid foundation for future systematic investigations. Here, we reinforced previous findings that the genus *Beilschmiedia* is polyphyletic (Rohwer et al., 2014). We also identified that *Beilschmiedia* is subdivided into at least six groups: i) an African species group closely related to *Potameia*, ii) a paraphyletic Australasian species group closely related to *Endiandra*, iii) a core *Beilschmiedia* group containing Asian *Beilschmiedia* plus one Neotropical lineage (represented by *B. brenesii*), iv) a Neotropical group represented by *B. immersinervis*, v) *B. turbinata*, and vi) *B. glauca*. Neotropical species thus constitute at least two separate clades, one that is closely related to Asian *Beilschmiedia*, and the other that is sister to a clade containing core *Beilschmiedia*, *Sinopora*, and *Syndiclis*.

Our findings merit a re-evalution of taxonomic characters that have been traditionally used to delimit subgroups within the *Beilschmiedia* group. This has involved the size and distribution of the terminal buds, which fall into two categories recognized by Hooker (1886) at the sectional rank. The first bud type is small and usually pubescent, e.g., *B. pauciflora*, *B. yunnanensis*, and *B. tsangii* Merr. In light of our findings that *Beilschmiedia* is not monophyletic, it is perhaps unsurprising that other genera of the *Beilschmiedia* group possess similar terminal buds, e.g., *Syndiclis*, *Hexapora*, and *Endiandra*. The second bud type is big, ovoid, plump, and usually glabrous, and includes a number of Asian species, e.g., *B. intermedia* C.K. Allen, *B. erythrophloa* Hayata, *B. robusta*, and *B. percoriacea* C. K. Allen, etc. Hooker (1886) speculated that species with big and glabrous terminal buds might merit generic status. Several previous phylogenetic studies (Liu, 2013; Liu et al., 2013) have

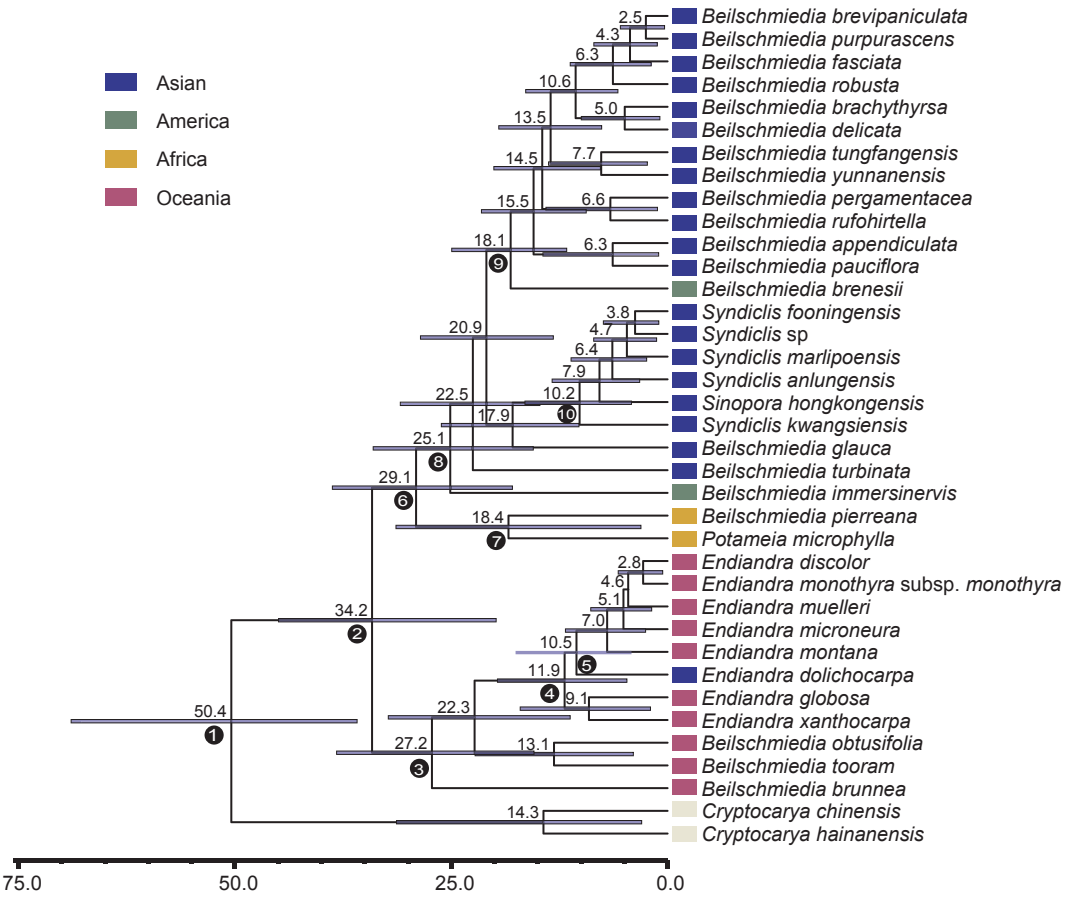

Fig. 3. Time-tree of the *Beilschmiedia* group from the time tree of Lauraceae. Numbers in black circles indicating important divergence events within the *Beilschmiedia* group.

Table 6
Divergence time of major nodes of the *Beilschmiedia* group using BEAST.

Node	Mean age (Ma)	95% HPD (Ma)
1	50.4	35.9–68.9
2	34.2	19.8–45.0
3	27.2	15.4–38.3
4	11.9	4.7–19.7
5	10.5	4.2–17.6
6	29.1	17.9–38.7
7	18.4	3.1–31.4
8	25.1	15.5–34.0
9	18.1	11.6–25.0
10	10.2	4.1–16.4

Note: node numbers correspond to those in the time tree of the *Beilschmiedia* group (Fig. 3).

supported the monophyly of species with big buds, supporting Hooker's suspicion. Our plastid phylogeny corroborates these findings and indicate that the four species with big terminal buds constitute a robust clade, including *B. robusta*, *B. fasciata*, *B. purpurascens*, and *B. brevipaniculata* (Fig. 2). In light of these results, large buds might have taxonomic utility, but small buds are likely homoplastic and not useful for delimiting major clades of *Beilschmiedia* sensu stricto.

4.2. Taxonomic delimitation of Endiandra

Species of *Endiandra* are distributed from southern China to Australia (Hyland, 1989; Li et al., 2008a). Traditionally, the genus had been delimited mainly by its flowers, which bear three stamens. A few species, however, possess exceptional stamen numbers: *E. xanthocarpa* has two stamens, whereas *E. montana* and *E. globosa* possess six stamens (Hyland, 1989). Allen (1942) established *Brassiodendron* based on a species with six stamens, viz. *Brassiodendron fragrans*. At that time, she was presumably unaware that the same species had been described earlier as *Endiandra montana*. Hyland (1989) subsequently proposed returning *Brassiodendron* to *Endiandra* based on overall morphological similarity. Rohwer (1993), however, felt that *Brassiodendron* should be maintained as distinct and placed this genus together with *Beilschmiedia*, *Hexapora,* and *Endiandra* in the *Beilschmiedia* group. In our plastid phylogeny, all *Endiandra* species, including those unusual species with exceptional stamen number, form a well-supported clade. These findings support the taxonomic hypotheses by Hyland (1989) and van der Werff and Nishida (2010) that *Brassiodendron* be synonymized under *Endiandra*.

4.3. Relationships of Syndiclis and Sinopora

Hooker (1886) established *Syndiclis* when he noticed that the type species *S. paradoxa* Hook. f. possessed anthers with one locule. Later, uni- versus bi-locular anthers were found to co-exist in a single species and it was hypothesized that uni-locular anthers were derived from the developmental fusion of two locules (Kostermans, 1957; Li and Pai, 1982). Based on this observation, Kostermans (1957) and Rohwer (1993) proposed incorporating *Syndiclis* into the genus *Potameia*, emphasizing their dimerous flowers. Li and Pai (1982), however, insisted on separating *Syndiclis* from *Potameia* because of their difference in staminodes: four in *Syndiclis* versus two or none in *Potameia*. The relationship between *Potameia* and *Syndiclis*, however, has not previously been investigated owing to insufficient taxon sampling (Liu et al., 2013; Rohwer et al., 2014).

To our surprise, *Syndiclis* is not most closely related to *Potameia*, but instead is placed with *Sinopora* (Fig. 2). *Sinopora* was originally described as a species of *Syndiclis* (Xia et al., 2006), but was later elevated to a separate genus owing to its trimerous flowers (Li et al., 2008b). Floral merosity, however, is known to be extremely variable in Chinese *Syndiclis*: both trimerous and dimerous flower types exist within a single species (Zeng et al., 2017). Floral merosity is thus not a good character to distinguish *Syndiclis* from *Sinopora*. Our investigation suggests that numerous shared characters support the placement of *Sinopora* with Chinese *Syndiclis*, including semi-circular stomata, fine leaf reticulations without free veinlet endings, small type terminal buds, and larger globose fruits (Yang and Zhang, 2010; Yang et al., 2012). In short, it seems untenable to separate *Sinopora* from Chinese *Syndiclis* on morphological and phylogenetic grounds.

Despite these findings, systematic relationships of the *Sinopora-Syndiclis* clade remain uncertain. Rohwer et al. (2014) suggested that *Sinopora* is sister to a Central American *Beilschmiedia* clade including *B. immersinervis*, but with low support (BS $<$ 50, PP $>$ 0.9). Further studies are necessary to determine the phylogenetic relationships of the *Sinopora-Syndiclis* clade.

4.4. Recent diversification of the Beilschmiedia group

Our divergence time estimates are largely congruent with previous studies, where comparable (Chanderbali et al., 2001; Li et al., 2011). One substantial disagreement between our divergence times and those of Chanderbali et al. (2001), however, regards the split between the *Beilschmiedia* group and *Cryptocarya* (~50 vs. 90 Ma). Based on their older age estimates, Chanderbali et al. (2001) hypothesized that the genus *Beilschmiedia* was ancient and widespread on Gondwanan land fragments when at least Africa and South America were nearly connected or only recently fragmented. They also hypothesized that the Asian distribution of *Beilschmiedia* was due to the rafting of the Indian subcontinent prior to its collision into the Asian subcontinent. Our results suggest much more recent estimates for these events and indicate that the *Beilschmiedia* group diverged from *Cryptocarya* in the Early Eocene (~50 Ma), and subsequently split into two large subclades around the Eocene − Oligocene boundary (~34 Ma) during periods of global cooling (Zachos et al., 2001). Such a finding renders the Gondwanan history outlined by Chanderbali et al. (2001) unlikely. Our age estimates are much more recent than the separation of western Gondwana, which is inferred to have been completed by the Late Cretaceous (Scotese et al., 1988; Hay et al., 1999; Upchurch, 2008). Taken together, the inferred recent diversification of the *Beilschmiedia* group is in accordance with numerous studies indicating that many pantropical distributions are not due to vicariance of the Gondwanan supercontinent but rather to more recent dispersal (e.g., Davis et al., 2002; Ruhfel et al., 2016; Beaulieu et al., 2013).

Lastly, the migration of *Beilschmiedia* between Asia and the Americas is thought to have occurred more than once (Rohwer et al., 2014). Our analyses support this hypothesis: we identified two recent divergence events involving Central American and Asian *Beilschmiedia* species. *Beilschmiedia immersinervis* represents the oldest such instances, its divergence from Asian species occurred in the latest Oligocene ~25 Ma, whereas *B. brenesii* represents a younger instance, and appears to have diverged from its Asian relatives ~18 Ma during the Mid-Miocene Climatic Optimum (Song et al., 2018). What might explain the distribution of these close relatives that span the New and Old Worlds? Floristic exchange between the New World and Asia via Beringian connections seems unlikely in the Neogene owing to the mostly tropical affinities of Lauraceae (Donoghue et al., 2001; Tiffney and Manchester, 2001). Most disjunctions of this nature in Lauraceae have instead been attributable to boreotropical migrations via high-latitude land connections involving the north Atlantic, e.g., *Caryodaphnopsis* Airy Shaw (Li et al., 2016b), *Cinnamomum* Schaeff. (Huang et al., 2016), and the *Persea* group (Li et al., 2011). Some of these hypothesized migratory events would have undoubtedly involved longer distance dispersal as continental land connections became increasingly fragmented (Davis et al., 2002, 2004; Li et al., 2011). Our study reinforces this idea and implies that more recent Neogene migration may be important in shaping *amphi*-Pacific tropical distributions in the *Beilschmiedia* group. Previous studies have proposed that fruit-eating birds may contribute to the dispersal of large seeded *Beilschmiedia* (Wotton, 2007; Kelly et al., 2010), but further investigations are required to clarify dispersal mechanisms within this group.

4.5. Future directions

Our study applied broad taxonomic sampling to resolve the backbone phylogeny of the *Beilschmiedia* group, and provided a coarse timeline of its divergence to motivate future biogeographic investigations. Our effort to resolve the major outline of the *Beilschmiedia* group phylogeny and clarify intergenic relationships was largely accomplished. Despite our efforts, we acknowledge key sampling gaps, especially in our geographical sampling, that should be improved in future investigations. The *Beilschmiedia* group contains $>$ 400 species worldwide (Plants of the World Online, http://powo.science.kew.org/), and our study included ~8% of its total species (Table S2). In particular, the *Beilschmiedia* group has over 100 species in Africa (Table S2). Our sampling included only two representative species from within this key geographical region. We were also unable to sample key species from southern South America to better represent neotropical species diversity (Rohwer et al., 2014). Finally, more than 100 species of the *Beilschmiedia* group occur in southeastern Asia, and were not well represented in our study. In particular, the monotypic *Hexapora* from this region was not included. This genus may be extinct in the wild because it has not been collected for over 100 years according to a recent revision of the genus (de Kok, 2016). Herbarium tissues may be our only hope for sampling this species.

CRediT authorship contribution statement

Haiwen Li: Data curation, Writing - original draft, Writing - review & editing. **Bing Liu:** . **Charles C. Davis:** Conceptualization, Methodology, Writing - review & editing, Supervision. **Yong Yang:** Conceptualization, Methodology, Writing - original draft, Writing - review & editing, Supervision.

Declaration of Competing Interest

The authors declare that they have no known competing financial interests or personal relationships that could have appeared to influence the work reported in this paper.

Acknowledgements

We thank Henk van der Werff & Jim Solomon of Missouri Botanical Garden for a number of DNA samples of the *Beilschmiedia* group, to Jens G. Rohwer and Jie Li for their valuable suggestions on our manuscript. Thanks are also due to Dr. Y. Song of Xishuangbanna Tropical Botanical Garden for availability of 34 plastomes of the Laurales including *B. turbinata* Bing Liu & Y. Yang, *B. robusta* C. K. Allen, *E. dolichocarpa* S.K. Lee & Y.T. Wei, *E. muelleri* Meisn., *S. anlungensis* H.W. Li, and *S. marlipoensis* H.W. Li.

Funding

This work was supported by the National Natural Science Foundation of China [31970205, 31470301, 31770211], and the China Scholarship Council.

Author contributions

YY & BL conceived the idea; YY & CCD designed the research; BL and YY collected DNA materials; HWL conducted the experiment and data analyses; and HWL, YY, and CD prepared and revised the manuscript.

Appendix A. Supplementary material

Supplementary data to this article can be found online at https://doi.org/10.1016/j.ympev.2020.106901.

References

Akaike, H., 1973. Information theory as an extension of the maximum likelihood principle. In: Petrov, B.N., Csaki, F. (Eds.), Second International Symposium on Information Theory. Akademiai Kiado, Budapest, Hungary, pp. 267–281.

Allen, C.K., 1942. Studies in the Lauraceae, IV. Preliminary study of the Papuasian species collected by the Archbold expeditions. J. Arn. Arb. 23, 133–155.

Arifiani, D., 2001. Taxonomic revision of *Endiandra* (Lauraceae) in Borneo. Blumea 46, 99–124.

Atkinson, B.A., Stockey, R.A., Rothwell, G.W., Mindell, R.A., Bolton, M.J., 2015. Lauraceous Flowers from the Eocene of Vancouver Island: *Tinaflora beardiae* gen. et sp. nov. (Lauraceae). Int. J. Plant Sci. 176, 567–585.

Bankevich, A., Nurk, S., Antipov, D., Gurevich, A.A., Dvorkin, M., Kulikov, A.S., Lesin, V.M., Nikolenko, S.I., Pham, S., Prjibelski, A.D., Pyshkin, A.V., Sirotkin, A.V., Vyahhi, N., Tesler, G., Alekseyev, M.A., Pevzner, P.A., 2012. SPAdes: a new genome assembly algorithm and its applications to single-cell sequencing. J. Comput. Biol. 19, 455–477.

Beaulieu, J.M., Tank, D.C., Donoghue, M.J., 2013. A Southern Hemisphere origin for campanulid angiosperms, with traces of the break-up of Gondwana. BMC Evol. Biol. 13, 80. http://www.biomedcentral.com/1471-2148/13/80.

Chanderbali, A.S., van der Werff, H., Renner, S.S., 2001. Phylogeny and historical biogeography of Lauraceae: evidence from the chloroplast and nuclear genomes. Ann. MO Bot. Gard. 88, 104–134.

Chen, C.H., Zheng, Y.J., Liu, S., Zhong, Y.D., Wu, Y.F., Li, J., Xu, L.A., Xu, M., 2017. The complete chloroplast genome of Cinnamomum camphora and its comparison with related Lauraceae species. PeerJ 5, e3820; doi 10.7717/peerj.3820.

Davis, C.C., Bell, C.D., Mathews, S., Donoghue, M.J., 2002. Laurasian migration explains Gondwanan disjunctions: evidence from Malpighiaceae. Proc. Nat. Acad. Sci., USA 99, 6833–6837.

Davis, C.C., Fritsch, P.W., Bell, C.D., Mathews, S., 2004. High latitude Tertiary migrations of an exclusively tropical clade: evidence from Malpighiaceae. Int. J. Plant Sci. 165, S107–S121.

de Kok, R.P.J., 2016. Notes on the monotypic genus *Hexapora* (Lauraceae), endemic to Peninsular Malaysia. Gard. Bull. Singapore 68, 201–208.

Donoghue, M.J., Bell, C.D., Li, J.H., 2001. Phylogenetic patterns in Northern Hemisphere plant geography. Int. J. Plant Sci. 162 (6 Suppl.), S41–S52.

Doyle, J., Endress, P.K., 2010. Integrating Early Cretaceous fossils into the phylogeny of living angiosperms: Magnoliidae and eudicots. J. Syst. Evol. 48, 1–35.

Doyle, J.A., Endress, P.K., Upchurch, G.R., 2008. Early Cretaceous monocots: a phylogenetic evaluation. Acta Musei. Nat. Pragae Ser. B - Hist. Nat. 64, 61–89.

Drummond, A.J., Suchard, M.A., Xie, D., Rambaut, A., 2012. Bayesian phylogenetics with BEAUti and the BEAST 1.7. Mol. Biol. Evol. 29, 1969–1973.

Eklund, H., 2000. Lauraceae flowers from the Late Cretaceous of North Carolina, U.S.A. Bot. J. Linn. Soc. 132, 397–428.

Friis, E.M., Eklund, H., Pedersen, K.R., Crane, P.R., 1994. *Virginianthus calycanthoides* gen. et sp. nov. —A calycanthaceous flower from the Potomac Group (Early Cretaceous) of eastern North America. Int. J. Plant Sci. 155, 772–785.

Gentry, A.H., 1988. Changes in plant community diversity and floristic composition on environmental and geographical gradients. Ann. MO Bot. Gard. 75, 1–34.

Gitzendanner, M.A., Soltis, P.S., Yi, T.S., Li, D.Z., Soltis, D.E., 2018. Plastome phylogenetics: 30 years of inferences into plant evolution. Adv. Bot. Res. 85, 293–313.

Hay, W.W., DeConto, R.M., Wold, C.N., Wilson, K.M., Voigt, S., Schulz, M, Wold, A.R., Dullo, W.C., Ronov, A.B., Balukhovsky, A.N., Söding, E., 1999. Alternative global Cretaceous paleogeography. In: Barrera, E., Johnson, C.C. (Eds.), Evolution of the Cretaceous Ocean-Climate System: Boulder, Colorado, Geological Society of America Special Paper 332, pp 1–47. doi: 10.1130/0-8137-2332-9.1.

Hooker, J.D., 1886. The Flora of British India, vol. 5, Chenopodiaceae to Orchideae. L. Reeve, London, UK.

Huang, D.I., Cronk, Q.C., 2015. Plann: A command-line application for annotating plastome sequences. Appl. Plant Sci. 3 apps.1500026.

Huang, J.F., Li, L., van der Werff, H., Li, H.W., Rohwer, J.G., Crayn, D.M., Meng, H.H., van der Merwe, M., Conran, J.G., Li, J., 2016. Origins and evolution of cinnamon and camphor: A phylogenetic and historical biogeographical analysis of the *Cinnamomum* group (Lauraceae). Mol. Phylogenet. Evol. 96, 33–44.

Hyland, B.P.M., 1989. A revision of Lauraceae in Australia (excluding *Cassytha*). Austr. Syst. Bot. 2, 135–367.

Katoh, K., Standley, D.M., 2013. MAFFT multiple sequence alignment software version 7: improvements in performance and usability. Mol. Biol. Evol. 30, 772–780.

Kearse, M., Moir, R., Wilson, A., Stones-Havas, S., Cheung, M., Sturrock, S., Buxton, S., Cooper, A., Markowitz, S., Duran, C., Thierer, T., Ashton, B., Meintjes, P., Drummond, A., 2012. Geneious Basic: an integrated and extendable desktop software platform for the organization and analysis of sequence data. Bioinformatics 28, 1647–1649.

Kelly, D., Ladley, J.J., Robertson, A.W., Anderson, S.H., Wotton, D.M., Wiser, S.K., 2010. Mutualisms with the wreckage of an avifauna: the status of bird pollination and fruit dispersal in New Zealand. New Zealand J. Ecol. 34, 66–85.

Kochummen, K.M., 1989. Lauraceae. In: Ng, F.S.P. (Ed.), Tree Flora of Malaya A Manual for Foresters, vol. 4. Longman, Kuala Lumpur, Malaysia, pp. 98–178.

Kondraskov, P., Schütz, N., Schüßler, C., de Sequeira, M.M., Guerra, A.S., Caujapé-Castells, J., Jaén-Molina, R., Marrero-Rodríguez, A., Koch, M.A., Linder, P., Kovar-Eder, J., Thiv, M., 2015. Biogeography of Mediterranean hotspot biodiversity: re-evaluating the 'Tertiary Relict' hypothesis of Macaronesian laurel forests. PLoS ONE 10 (7), e0132091. https://doi.org/10.1371/journal.pone.0132091.

Kostermans, A.J.G.H., 1957. Lauraceae. Reinwardtia 4 (2), 193–256.

Kurtz, S., Choudhuri, J.V., Ohlebusch, E., Schleiermacher, C., Stoye, J., Giegerich, R., 2001. REPuter: the manifold applications of repeat analysis on a genomic scale. Nucleic Acids Res. 29 (22), 4633–4642.

Li, H.W., Pai, P.Y., 1982. Syndiclis. In: Li, H.W. (Ed.), Flora Reipublicae Popularis Sinicae, vol. 31, Lauraceae and Hernandiaceae. Science Press, Beijing, China, pp. 152–160.

Li, J., Christophel, D.C., Conran, J.G., Li, X.W., 2004. Phylogenetic relationships within the 'core' Laureae (*Litsea* complex, Lauraceae) inferred from sequences of the chloroplast gene matK and nuclear ribosomal DNA ITS regions. Plant Syst. Evol. 246, 19–34.

Li, J., Xia, N.H., Li, X.W., 2008a. *Sinopora*, a new genus of Lauraceae from South China. Novon 18, 199–201.

Li, J.Z., Qiu, J., Liao, W.B., Jin, J.H., 2009. Eocene fossil *Alseodaphne* from Hainan Island of China and its paleoclimatic implications. Sci. China Ser. D-Earth Sci. 52, 1537–1542. https://doi.org/10.1007/s11430-009-0120-1.

Li, L., Li, J., Rohwer, J.G., van der Werff, H., Wang, Z.H., Li, H.W., 2011. Molecular phylogenetic analysis of the "*Persea*" group (Lauraceae) and its biogeographic implications on the evolution of tropical and subtropical amphi-Pacific disjunctions. Amer. J. Bot. 98, 1520–1536.

Li, L., Madriñán, S., Li, J., 2016a. Phylogeny and biogeography of *Caryodaphnopsis* (Lauraceae) inferred from low-copy nuclear gene and ITS sequences. Taxon 65, 433–443.

Li, Y.G., Xu, W.Q., Zou, W.T., Jiang, D.Y., Liu, X.H., 2017. Complete chloroplast genome sequences of two endangered *Phoebe* (Lauraceae) species. Bot. Stud. 58, 37. https://doi.org/10.1186/s40529-017-0192-8.

Li, Y.X., Jiao, W.J., Liu, Z.H., Jin, J.H., Wang, D.H., He, Y.X., Quan, C., 2016b. Terrestrial responses of low-latitude Asia to the Eocene-Oligocene climate transition revealed by integrated chronostratigraphy. Clim. Past 12, 255–272. https://doi.org/10.5194/cp-12-255-2016.

Li, X.W., Li, J., van der Werff, H., 2008b. *Endiandra* R. Brown, *Beilschmiedia* Nees, *Sinopora* J. Li et al., *Syndiclis* J.D. Hooker. In: In: Wu, Z.Y., Raven, P.R. (Eds.), Flora of China, vol. 7. Science Press, Beijing, China, pp. 231–247.

Liao, Q., Ye, T.H., Song, Y., 2018. Complete chloroplast genome sequence of a subtropical tree, *Parasassafras confertiflorum* (Lauranceae). Mitochondrial DNA B 3, 1216–1217. https://doi.org/10.1080/23802359.2018.1532331.

Liu, B., 2013. Systematics and Biogeography of the Subtribe Beilschmiediineae (Lauraceae) in China. Ph.D. thesis. Institute of Botany, the Chinese Academy of Sciences, Beijing, China.

Liu, B., Yang, Y., Xie, L., Zeng, G., Ma, K.P., 2013. *Beilschmiedia turbinata*: a newly recognized but dying species of Lauraceae from tropical Asia based on morphological and molecular data. PLoS ONE 8 (6), e67636.

Lohse, M., Drechsel, O., Kahlau, S., Bock, R., 2013. OrganellarGenomeDRAW–a suite of tools for generating physical maps of plastid and mitochondrial genomes and visualizing expression data sets. Nucleic Acids Res. 41 (Web Server issue), W575–W581.

Massoni, J., Doyle, J., Sauquet, H., 2015. Fossil calibration of Magnoliidae, an ancient lineage of angiosperms. Palaeontol. Electron. 18.1.2FC; 1–25; palaeo-electronica.org/content/fc-2.

Ning, Y.Y., Xing, F.W., 2014. Preliminary evaluation and screening of non-food biodiesel plant resources of Lauraceae in China. Plant Sci. J. 32, 279–288.

Nishida, S., 1999. Revision of *Beilschmiedia* (Lauraceae) in the Neotropics. Ann. MO Bot. Gard. 86, 657–701.

Nylander, J.A.A. 2004. MrModeltest, version 2. Program distributed by the author. Evolutionary Biology Centre, Uppsala University, Sweden.

Rambaut, A., 2009. FigTree v.1.4. Available at: < http://tree.bio.ed.ac.uk/software/figtree/ > .

Renner, S.S., 2004. Variation in diversity among Laurales, Early Cretaceous to present. Biol. Skr. 55, 441–458.

Richter, H.G., 1981. Anatomie des sekundären Xylems und der Rinde der Lauraceae. Sonderb. Naturwiss. Vereins, Hamburg 5, 1–148.

Rohde, R., Rudolph, B., Ruthe, K., Lorea-Hernandez, F.G., de Moraes, P.L.R., Rohwer, J.G., 2017. Neither *Phoebe* nor *Cinnamomum* – the tetrasporangiate species of *Aiouea* (Lauraceae). Taxon 66, 1085–1111.

Rohwer, J.G., 1993. Lauraceae. In: Kubitzki, K., Rohwer, J.G., Bittrich, V. (Eds.), The Families and Genera of Vascular Plants, vol. 2, Flowering Plants: Dicotyledons Magnoliid, Hamamelid and Caryophyllid Families. Springer-Verlag, Berlin, Germany, pp. 366–390.

Rohwer, J.G., 2000. Toward a phylogenetic classification of the Lauraceae: evidence from *matK* sequences. Syst. Bot. 25, 60–71.

Rohwer, J.G., de Moraes, P.L.R., Rudolph, B., van der Werff, H., 2014. A phylogenetic analysis of the *Cryptocarya* group (Lauraceae), and relationships of *Dahlgrenodendron*, *Sinopora*, *Triadodaphne*, and *Yasunia*. Phytotaxa 158, 111–132.

Rohwer, J.G., Rudolph, B., 2005. Jumping genera: the phylogenetic positions of *Cassytha*,

Hypodaphnis, and *Neocinnamomum* (Lauraceae) based on different analyses of *trnK* intron sequences. Ann. MO Bot. Gard. 92, 153–178.
Rozas, J., Ferrer-Mata, A., Sanchez-DelBarrio, J.C., Guirao-Rico, S., Librado, P., Ramos-Onsins, S.E., Sanchez-Gracia, A., 2017. DnaSP 6: DNA Sequence Polymorphism Analysis of Large Data Sets. Mol. Biol. Evol. 34, 3299–3302.
Ruhfel, B.R., Bove, C.P., Philbrick, C.T., Davis, C.C., 2016. Dispersal largely explains the Gondwanan distribution of the ancient tropical clusioid plant clade. Amer. J. Bot. 103, 1117–1128.
Scotese, C.R., Gahagan, L.M., Larson, R.L., 1988. Plate tectonic reconstructions of the Cretaceous and Cenozoic ocean basins. Tectonophysics 155, 27–48.
Song, Y., Yao, X., Tan, Y.H., Gan, Y., Yang, J.B., Corlett, R.T., 2017a. Comparative analysis of complete chloroplast genome sequences of two subtropical trees, *Phoebe sheareri* and *Phoebe omeiensis* (Lauraceae). Tree Genet. Genomes 13, 120.
Song, Y., Yu, W.B., Tan, Y.H., Jin, J.J., Wang, B., Yang, J.B., Liu, B., Corlett, R.T., 2019. Plastid phylogenomics improve phylogenetic resolution in the Lauraceae. J. Syst. Evol. https://doi.org/10.1111/jse.12536.
Song, Y., Yu, W.B., Tan, Y.H., Liu, B., Yao, X., Jin, J.J., Padmanaba, M., Yang, J.B., Corlett, R.T., 2017b. Evolutionary comparisons of the chloroplast genome in lauraceae and insights into loss events in the Magnoliids. Genome Biol. Evol. 9, 2354–2364.
Song, Y., Yao, X., Tan, Y.H., Gan, Y., Corlett, R.T., 2016. Complete chloroplast genome sequence of the avocado: gene organization, comparative analysis, and phylogenetic relationships with other Lauraceae. Canadian J. Forest Res. 46, 1293–1301.
Song, Y.G., Wang, Q.S., An, Z.S., Qiang, X.K., Dong, J.B., Chang, H., Zhang, M.S., Guo, X.H., 2018. Mid-Miocene climatic optimum: clay mineral evidence from the red clay succession, Longzhong Basin, Northern China. Palaeogeogr. Palaeoclimatol. Palaeoecol. 512, 46–55.
Sri-Ngernyuang, K., Kanzaki, M., Mizuno, T., Noguchi, H., Teejuntuk, S., Sungpalee, C., Hara, M., Yamakura, T., Sahunalu, P., Dhanmanonda, P., Bunyavejchewin, S., 2003. Habitat differentiation of Lauraceae species in a tropical lower montane forest in northern Thailand. Ecol. Res. 18, 1–14.
Tang, B., Han, M., Xu, Q.Q., Jin, J.H., 2016. Leaf cuticle microstructure of *Machilus maomingensis* sp. nov. (Lauraceae) from the Eocene of the Maoming Basin, South China. Acta Geol. Sin. (English Ed.) 90, 1561–1571.
Tiffney, B.H., Manchester, S.R., 2001. The use of geological and paleontological evidence in evaluating plant phylogenetic hypotheses in the Northern Hemisphere Tertiary. Int. J. Pl. Sci. 162, S3–S17.
Upchurch, P., 2008. Gondwanan break-up: legacies of a lost world? Trends Ecol. Evol. 23, 229–236.
van der Werff, H., 1991. Studies in Malagasy Lauraceae I: novelties in Potameia. Adansonia sér. 4 13(3–4), 173–177.
van der Werff, H., 2001. An annotated key to the genera of Lauraceae in the Flora of Malesiana Region. Blumea 46, 125–140.
van der Werff, H., Nishida, S., 2010. *Yasunia* (Lauraceae), a new genus with two species from Ecuador and Peru. Novon 20, 493–502.
van der Werff, H., Richter, H.G., 1996. Toward an improved classification of Lauraceae. Ann. MO Bot. Gard. 83, 409–418.
von Balthazar, M., Pedersen, K.R., Crane, P.R., Stampanoni, M., Friis, E.M., 2007. *Potomacanthus lobatus* gen. et sp. nov., a new flower of probable Lauraceae from the Early Cretaceous (Early to Middle Albian) of Eastern North America. Amer. J. Bot. 94, 2041–2053.
von Balthazar, M., Crane, P.R., Pedersen, K.R., Friis, E.M., 2011. New flowers of Laurales from the Early Cretaceous (Early to Middle Albian) of eastern North America. In: Wanntorp, L., Ronse de Craene, L.P. (Eds.), Flowers on the Tree of Life. Cambridge University Press, Cambridge, UK, pp. 46–84.
Wotton, D.M., 2007. Consequences of dispersal failure: kereru and large seeds in New Zealand. Ph.D. thesis. School of Biological Sciences, University of Canterbury.
Xia, N.H., Deng, Y.F., Yip, K.L., 2006. *Syndiclis hongkongensis* (Lauraceae), a new species from China. J. Trop. Subtrop. Bot. 14, 75–77.
Yang, Y., Zhang, L.Y., 2010. Venation pattern of *Syndiclis* Hook.f. and its related genera. J. Trop. Subtrop. Bot. 18 (6), 643–649.
Yang, Y., Zhang, L.Y., Liu, B., van der Werff, H., 2012. Leaf cuticular anatomy and taxonomy of *Syndiclis* (Lauraceae) and its allies. Syst. Bot. 37, 861–878.
Zachos, J., Pagani, M., Sloan, L.C., Thomas, E., Billups, K., 2001. Trends, rhythms, and aberrations in global climate 65 Ma to present. Science 292, 686–693.
Zeng, G., Liu, B., Ferguson, D.K., Rohwer, J.G., Yang, Y., 2017. Floral structure and ontogeny of *Syndiclis* (Lauraceae). PLoS ONE 12 (10), e0186358. https://doi.org/10.1371/journal.pone.0186358.
Zhang, G.F., He, S.Y., 2014. Ornamental tree species resources of Lauraceae and their application in horticulture. Modern Hort. 2014 (4), 26–28.
Zhang, Y.J., Li, D.Z., 2011. Advances in phylogenomics based on complete chloroplast genomes. Pl. Divers. Resour. 33, 365–375.
Zhao, M.L., Song, Y., Ni, J., Yao, X., Tan, Y.H., Xu, Z.F., 2018. Comparative chloroplast genomics and phylogenetics of nine *Lindera* species (Lauraceae). Sci. Rep. 8, 8844. https://doi.org/10.1038/s41598-018-27090-0.